Acoustic scattering characteristics of underwater buried oil pipeline

Acoustic scattering characteristics of underwater buried oil pipeline

Jiancheng Yin[1], Xiangyu You[1,2*], Yu Yao[1,2]

[1] School of Hydraulic and Environmental Engineering, Changsha University of Science & Technology, Changsha 410114, China
[2] Key Laboratory of Water-Sediment Sciences and Water Disaster Prevention of Hunan Province, Changsha 410114, China

Email: csust_yxy@csust.edu.cn

Abstract. With the development of offshore oil resources, subsea oil pipelines have emerged. As a fast, economical, and safe way to transport oil resources, subsea pipelines are known as the "lifeline" of offshore oil projects. However, the detection of submarine pipelines is very difficult due to the complex underwater environment. One of the mainstream methods to detect submarine pipelines is the employment of sonar. Hence, the acoustic scattering characteristics of submarine pipelines play an important role in detecting themselves. In this study, the acoustic scattering model of the buried pipeline is established using the finite element method, and the scattering mechanism of the buried pipeline is analyzed. The effects of different frequencies, grazing angles, burial depth, and other factors on the acoustic scattering characteristics of the buried pipeline are investigated, providing the reference significance for detecting submarine pipelines.

1. Introduction

Acoustic waves, as the mainstream means of transmitting signals in seawater, are of great importance in studying acoustic wave propagation in the complex seabed environment for the detection of submarine pipelines. The detection and identification of submerged mines, submarine pipelines, and submarine sediments is a significant problem in underwater detection technology, due to the superposition of the target echoes and strong background reverberation. The scattering waves and the transmission waves arising from the non-uniform seabed are the main factors affecting the identification of the scattering characteristics of the target. Therefore, more accurate physical models are needed to describe the physical properties of the sediment and the interaction of acoustic waves with the seafloor interface.

With the need for underwater target detection and the theoretical development of sediment modeling, many scholars have done a lot of work on sediment characterization and modeling, including sediment layer attenuation models, reflection and absorption models, and so on. Due to the complexity of the seafloor environment, the current understanding of underwater sediments is still very limited, and a lot of theoretical research and experimental comparisons are still needed[1].

Scientists have carried out a great deal of research into the acoustic properties of sediments, of which underwater sediment modeling based on the Biot theory has received greater attention and development[2]. Biot first proposed the theory describing porous media and saturated fluids in 1956 to simulate the propagation of acoustic waves through sediments. Biot's theory explains the phenomenon of elastic wave propagation in porous media and establishes a theoretical model of the sound propagation attenuation of the porous medium[3,4]. Based on the Biot's theory, Stoll introduces inter-particle contact

caused by the skeleton loss and established the Biot-Stoll model[5]. The Biot-Stoll model is a physical model describing the acoustic propagation law in seafloor sediments, which can well explain the acoustic velocity dispersion phenomenon in sediments and is in good agreement with the laboratory data in a certain frequency range[6].

In this paper, based on the Biot-Stoll porous medium model, some seabed medium parameters were analyzed using COMSOL Multiphysics, and the acoustic reflection and attenuation characteristics of the sandy seabed with different sediment types were investigated[7]. The numerical simulation of the acoustic scattering of pipelines buried in sediment was conducted based on the Biot-Stoll theory, and the effects of different grazing angles, frequencies, and burial depths on the acoustic scattering of the oil pipeline buried in sediment were investigated.

2. Influence of porous medium parameters on reflection coefficient and attenuation coefficient

2.1 Water-porous media coupling model

In this example, the water domain is modeled by employing the Helmholtz equations, and the sediment domain is modeled by using the Biot-Stoll theory. The computational model is shown in figure 1, the upper domain is water, the lower domain is porous elastic medium, and the porous medium parameters are adopted from the sediment parameters in ref.5 as shown in table 1. The upper and lower boundaries are set as the PML (perfected matched layer) to serve as the absorption layer. The width of the problem domain is defined as twice the considered wavelength, and the left and right boundaries are set as the floquet periodic boundaries to simulate periodic structures.

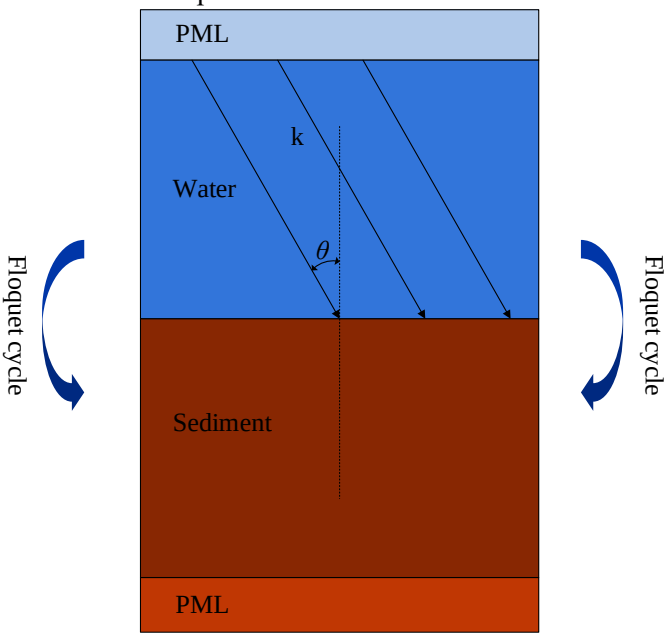

Figure 1. Computational model of water-porous medium

The acoustic wave impinges on the water-sediment interface with the incident angle θ, and the wave number can be defined as

$$\mathbf{k} = k_0[\sin(\theta), -\cos(\theta)]^{\mathrm{T}} \quad (1)$$

$$k_0 = \frac{\omega}{\mathrm{c}} \quad (2)$$

where ω is the angular frequency $2\pi f$. The incident plane wave can be expressed as

$$P_{in}(\mathbf{x}) = \mathrm{e}^{(-i(\mathbf{k}\cdot\mathbf{x}))} \quad (3)$$

$$\mathbf{x} = (x, y) \quad \text{.....(4)}$$

2.2 The influence of porous media parameters on reflection coefficient

The reflection sound fields under incident unit plane wave of different frequencies and incident angles were calculated for different sediment types (coarse sand, sandy mud, clayey mud). The reflection coefficient of sediment is defined as

$$R = \frac{P_{sc}}{P_{in}} \quad \text{.....(5)}$$

where P_{sc} denotes the amplitude of the reflection wave and P_{in} denotes the amplitude of the incident wave. The absolute values of the reflection coefficient R versus frequencies and incident angles are shown in figure 2 and figure 3, respectively.

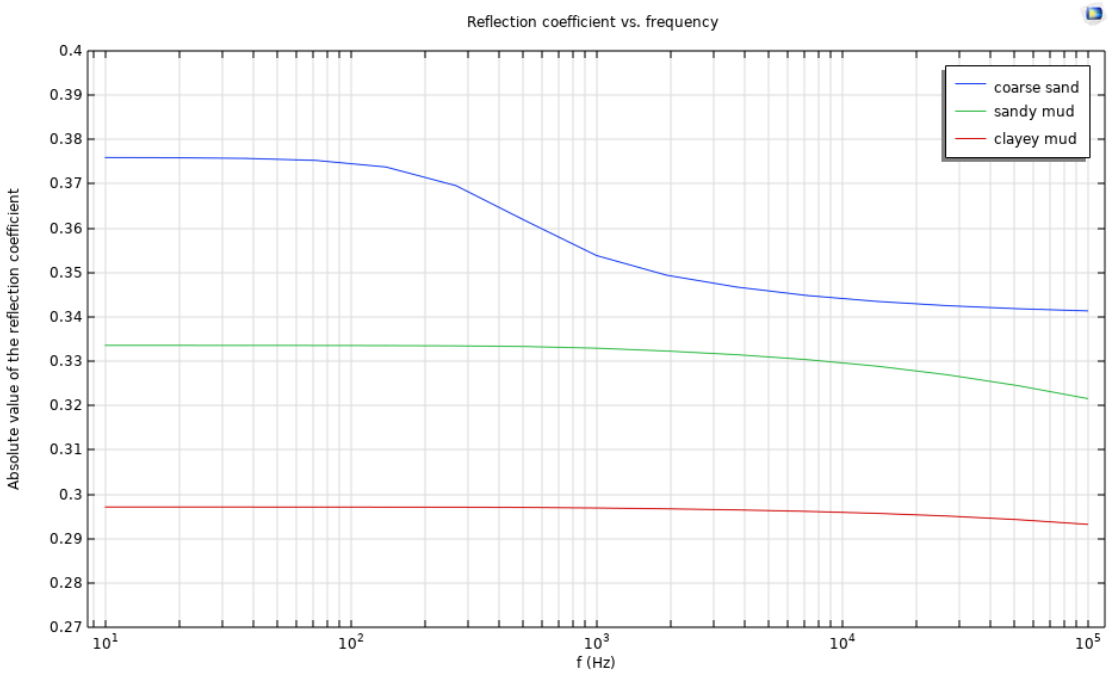

Figure 2. Reflection coefficient versus the frequencies at the incident angle of 90 degrees

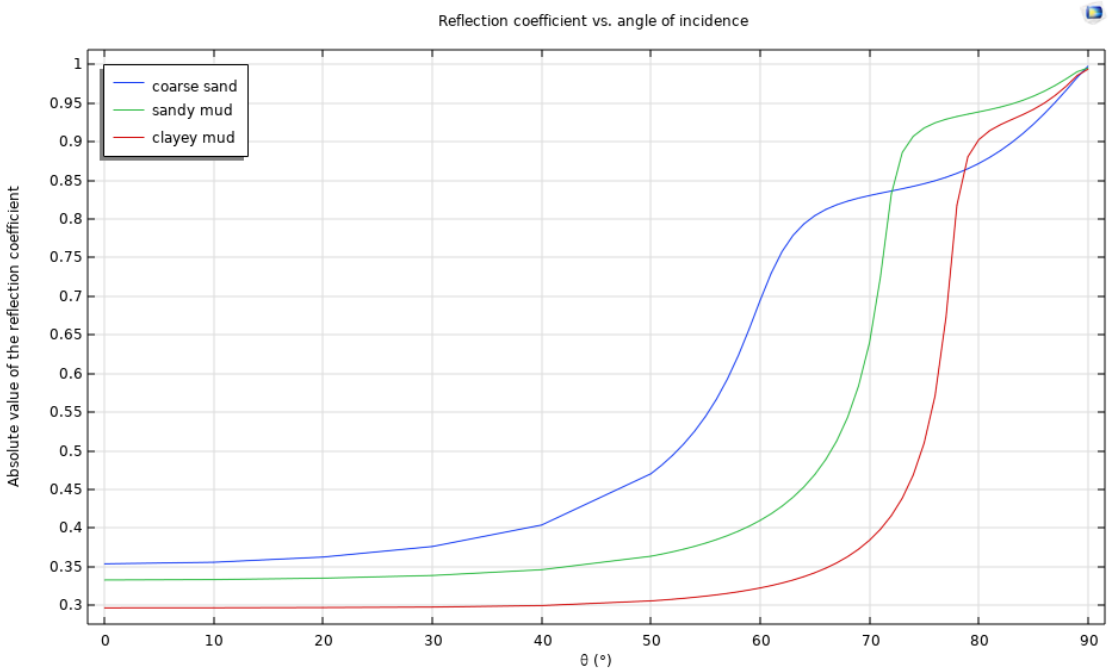

Figure 3. Reflection coefficient versus incident angles

In figure 2, when the incident angle of acoustic waves is vertical, the reflection coefficient decreases with increasing frequencies. In the frequency band of 10~100000 Hz, the reflection coefficient of coarse sand is the largest, the reflection coefficient of sandy mud is the second, and the smallest reflection coefficient is obtained from clayey mud. In addition, the reflection coefficient of coarse sand decreases very rapidly with the increase of frequencies.

Figure 3 shows the variation of the reflection coefficient with the incident angles at the calculated frequency of 1000 Hz. In the incident angles changing from 0 to 70°, the reflection coefficient of coarse sand is the largest, the reflection coefficient of sandy mud is the second, and the smallest reflection coefficient is obtained from clayey mud. For the incident angles between 70 and 90°, the reflection coefficients of sandy mud and clayey mud increase rapidly with increasing the incident angles, whereas the reflection coefficients of coarse sand increase more slowly.

2.3 Influence of porous media parameters on attenuation coefficient

The attenuation of acoustic wave will occur in the sediment to a certain degree, and the magnitude of attenuation is closely related to the incident wave frequency, porosity, and other parameters of the porous medium. The acoustic attenuation coefficient is defined by the following equation

$$\alpha = \frac{1}{x} 20 \lg \frac{A}{A_0} \quad \text{.....(6)}$$

where x is the distance from the source to the measurement point, A_0 is the sound pressure at the source, and A is the sound pressure at the measurement point. The variations of the acoustic attenuation coefficient of coarse sand, sandy mud, and clayey mud with the changing frequencies and incident angles are calculated. Figure 4 shows the attenuation coefficient versus frequencies at the vertical incident angle.

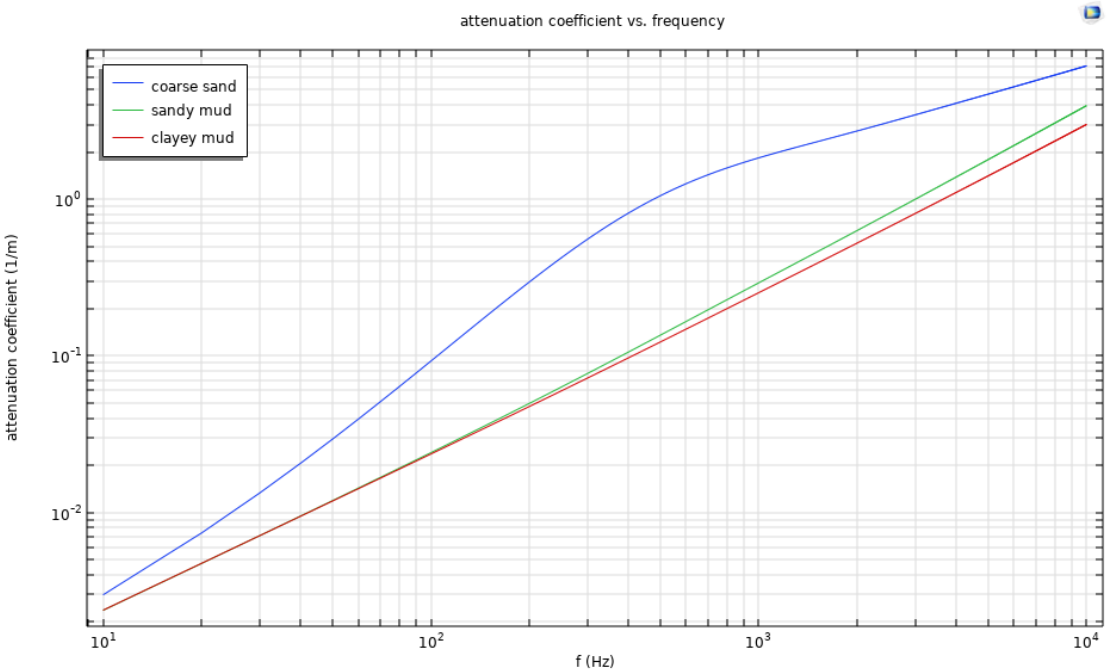

Figure 4. Attenuation coefficient versus the frequencies

As we can see, coarse sand has the largest attenuation coefficient, the attenuation coefficient of sandy mud is the second, and the smallest attenuation coefficient is obtained from clayey mud. In high frequencies, the attenuation coefficient of coarse sands grows fastest, the attenuation coefficient of sandy muds is the second, and the attenuation coefficient of clayey muds increases slowest.

3. Simulation of acoustic scattering of buried oil pipeline

3.1 Modelling of acoustic scattering of an underwater buried oil pipeline

The study of the acoustic scattering characteristics of buried objects usually includes various media such as water, sediments, and burials as shown in figure 5.

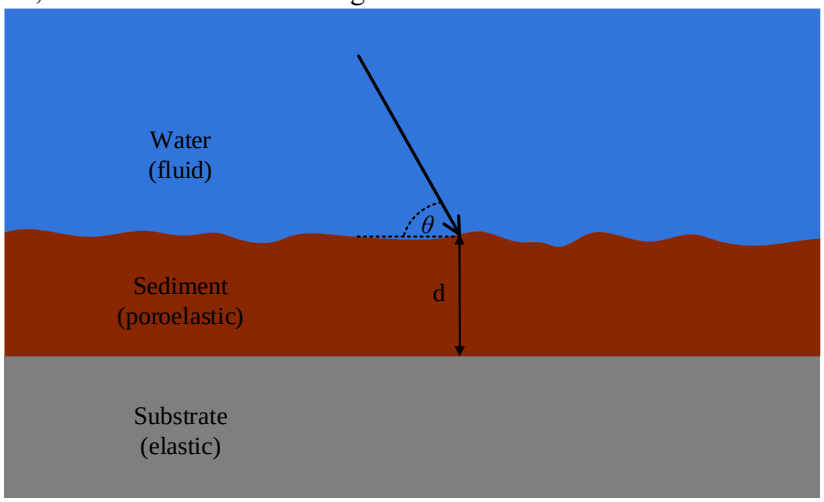

Figure 5. Real seabed environment

The substrate is located under the sediment and is far from the bottom of the water, therefore, it is not considered in this study. A typical computational model of acoustic scattering of an infinite buried oil pipeline is shown in figure 6.

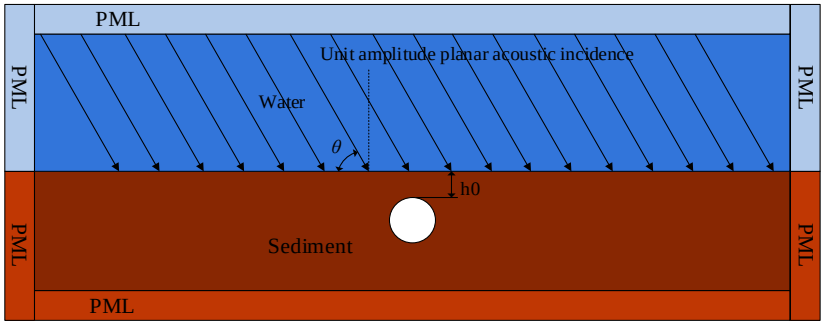

Figure 6. Modelling of acoustic scattering of the buried oil pipeline

The upper medium is water and the lower medium is the sediment simulated by the porous material. An oil-filled pipeline with a radius of 0.325 m and a thickness of 0.01 m is buried below the water-sediment interface, and the burial depth, h0, is the distance from the apex of the pipeline to the water-sediment interface. Besides, the computational domain is truncated using PML to serve as the absorption layer. The medium properties of the sandy sediment, cylinder, and crude oil are given in Table 1.

Table 1. Bunker and media parameters

symbolic	value	description
E	$2.1\cdot10^{11}$ Pa	Young's modulus of elastic materials
ν	0.3	Poisson's ratio for elastic materials
ρ_e	$7800\text{kg}/\text{m}^3$	Elastic material density
η	$1\cdot10^{-3}\,\text{Pa}\cdot\text{s}$	Fluid viscosity
ρ_f	$1000\text{kg}/\text{m}^3$	Fluid density
c_f	$1414\text{m}/\text{s}$	Fluid velocity of sound
β	0.47	Porosity
κ_p	$1\cdot10^{-10}\,\text{m}^2$	Permeability
ρ	$810\text{kg}/\text{m}^3$	Crude oil density
c	$1290\text{m}/\text{s}$	Crude oil velocity of sound
a	$4\cdot10^{-5}\,\text{m}$	Pore size parameter
τ	1.25	Tortuosity
K_b	$4.36\cdot10^7$ Pa	Frame bulk modulus
K_r	$3.6\cdot10^{10}$ Pa	Bulk modulus of grains
K_f	$2\cdot10^9$ Pa	Fluid bulk modulus
$\overline{K}_b$	(4.36E7 + 2.08E6i)Pa	Complex bulk modulus of the skeleton
μ	$2.61\cdot10^7$ Pa	Shear modulus of the skeleton
$\overline{\mu}$	(2.61E7 +1.24E6i)Pa	Complex shear modulus of the skeleton
ρ_s	$2650\text{kg}/\text{m}^3$	Skeleton solid particle density

To investigate the influence of different parameters on the acoustic scattering characteristics of the buried pipeline, the acoustic scattering fields with different grazing angles, burial depths, and pipeline radii are calculated based on the above model.

3.2 Influence of grazing angle on the acoustic scattering fields

The oil-filled pipeline is buried in the sediment at a depth of 0.25 m. The grazing angles of the incident plane wave were adopted as 30°, 45°, 60°, 75°, and 90°, and the monostatic acoustic scattering pressure at 1 m above the water-sediment interface is calculated here. The schematic diagram of the computational model is as shown in figure 7.

As shown in figure 8, the monostatic scattering pressure versus frequencies for the five observation point is plotted. The amplitude of scattering pressure at the corresponding observation point is maximum when the grazing angle is 90°, and is minimum when the grazing angle is 30°. As the grazing angle increases, the amplitude of scattering pressure at the observation points becomes larger. Therefore, a large grazing angle could be more favorable for pipeline detection, while a smaller grazing angle may make it more difficult to detect the pipeline.

Figure 9 gives the scattering pressure characteristics of the buried pipeline 1 meter from the center of the pipeline for different grazing angles at a fixed frequency of 2500 Hz. The directivity of the acoustic pressure of the pipeline is more obvious when the grazing angle is greater than 60 degrees, indicating that a larger grazing angle may be beneficial to obtain scattering signals with a larger signal-to-noise ratio, thus better identifying the pipelines.

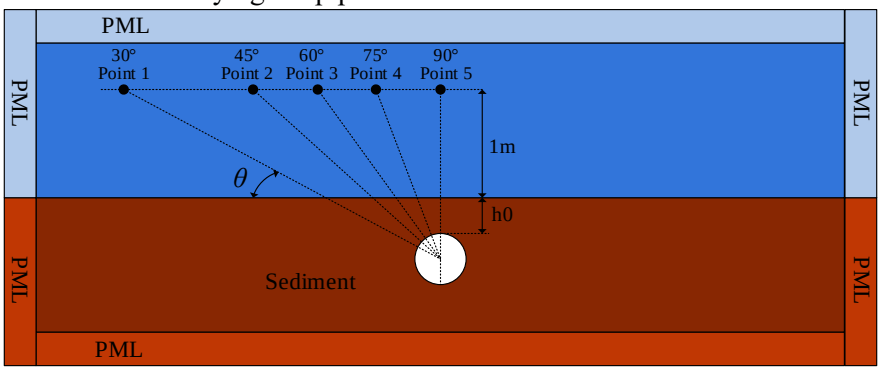

Figure 7. Schematic diagram of the location of the observation

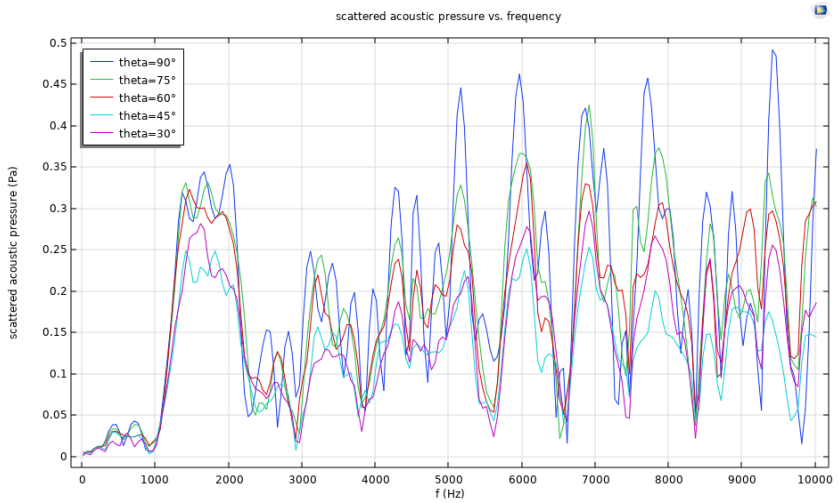

Figure 8. Monostatic scattering pressure at different observation points

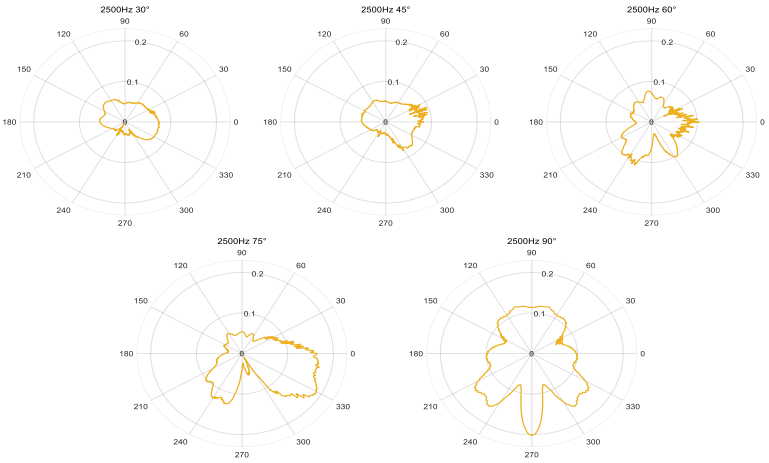

Figure 9. Scattering pressure characteristics of the buried pipeline 1 meter from the center of the pipeline

3.3 Influence of burial depth on the scattering pressure field

The oil-filled pipeline is buried with different depths in the sediment, and the burial depths h0 are set as 0.5, 1, and 1.5 m. The scattering pressure is obtained when the grazing angle of the incident wave is 90°.

As shown in figure 10, the larger the depth of the buried pipeline, the less scattering pressure the target scatters into the water, making it more difficult to detect the pipeline. Therefore, when the burial depth of the pipeline is 0.5m, the pipeline may be more easily detected.

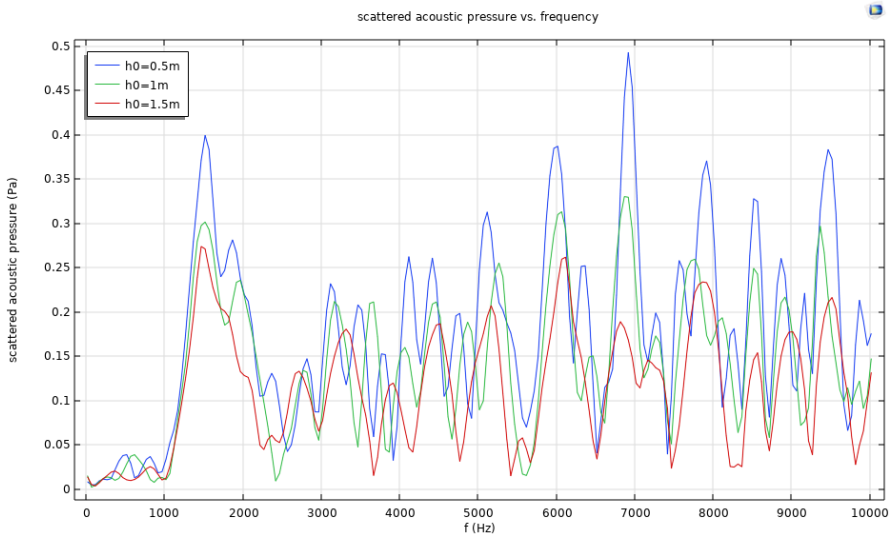

Figure 10. Scattering pressure of the buried pipeline at the grazing angle of 90 degrees for different burial depths

3.4 Influence of pipe radius on the scattering pressure

The two different oil-filled pipelines with a radius of 0.325 m and a thickness of 0.01 m, and a radius of 0.4 m and a thickness of 0.0175 m were buried at a depth of 0.25 m in the sediment. The scattering pressure at the measurement point 1 m above the water-sediment interface is calculated for the vertically incident plane wave.

As shown in figure 11, the amplitude of scattering pressure obtained at the measurement point is slightly greater for the pipe of 0.4m radius than that for the pipe of 0.325m radius. Therefore, larger radius pipes shall be easily detected than smaller radius pipes.

Figure 12 gives scattering pressure characteristics of the buried pipeline of different radii at a fixed frequency of 2500 Hz with a grazing angle of 90 degrees. It is obvious that the directivity of scattering

pressure of the large radius pipe is more prominent than that of the small radius pipe. Therefore, the large radius pipe can be easier to detect.

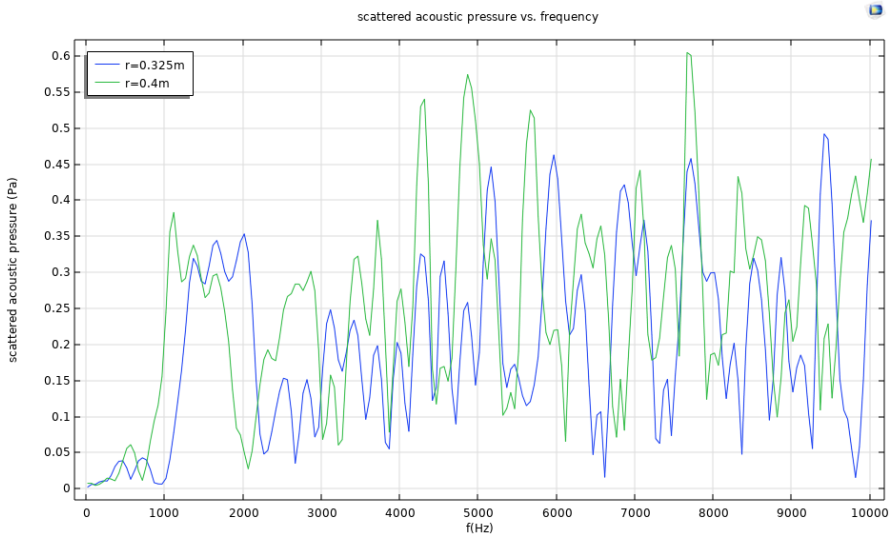

Figure 11. Scattering pressure at the grazing angle of 90 degrees for pipes of different radii

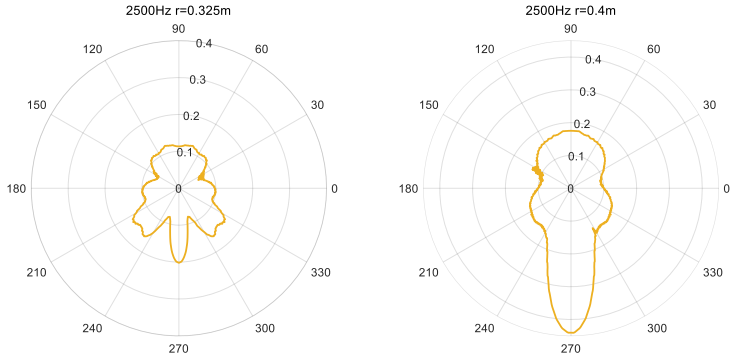

Figure 12. Scattering pressure characteristics of the buried pipeline of different radii

4. Conclusion

In this study, based on the water-porous medium coupling model, the reflection and attenuation coefficients of three types of sediments are parametrically analyzed. The numerical model of the buried oil pipeline is established to obtain the scattering pressure, and the acoustic scattering characteristics of the target under different burial conditions are analyzed. The larger grazing angle, smaller burial depth, and larger pipeline radius can be more favorable factors for pipeline detection, which is helpful to the daily inspection and maintenance of pipelines.

5. References

[1] Z. Zhao, Research on underwater buried object detection[D]. University of Electronic Science and Technology, 2017.

[2] C. Gong, W. Li and H. Jiang, Simulation and analysis of reflection coefficient of acoustic waves at seabed interface[J]. Ship Science and Technology, 2022, 44(16):126–29+133.

[3] Biot M A. Theory of deformation of a porous viscoelastic anisotropic solid[J]. Journal of Applied physics, 1956, 27(5): 459–467.

[4] Biot M A. Theory of propagation of elastic waves in a fluid-saturated porous solid. II. Higher

frequency range[J]. The Journal of the acoustical Society of america, 1956, 28(2): 179–191.
[5] Stoll R D and Kan T K. Reflection of acoustic waves at a water-sediment interface[J]. The Journal of the Acoustical Society of America, 1981, 70(1): 149–156.
[6] Thorsos E I, Williams K L and Chotiros N P, et al. An overview of SAX99: Acoustic measurements[J]. IEEE Journal of Oceanic Engineering, 2001, 26(1): 4–25.
[7] L. Peng, Y. Zhao and G. Yu, Reflection and refraction of acoustic waves at a water-porous sediment interface. [J]. Periodical of Ocean University of China, 2007, 37(4): 671–75.